Journal of Mechanical Engineering and Sciences (JMES)
ISSN (Print): 2289-4659; e-ISSN: 2231-8380
Volume 10, Issue 2, pp. 2065-2075, September 2016

DOI: https://doi.org/10.15282/jmes.10.2.2016.11.0195

# A study on bead-on-plate welding of AA7075 using low power fiber laser

**M.N.M. Salleh[1*], M. Ishak[1,2*], F.R.M. Romlay[1] and M.H. Aiman[1]**

[1]Faculty of Mechanical Engineering, Universiti Malaysia Pahang,
26600 Pekan, Pahang, Malaysia
[*]Email: mdnaqiuddinsalleh91@gmail.com; mahadzir@ump.edu.my
Phone: +6013-642 2261
[2]Automotive Engineering Centre, Universiti Malaysia Pahang,
26600 Pekan, Pahang, Malaysia

## ABSTRACT

Laser welding promises the best method to produce higher strength of aluminium joints compared to conventional arc welding process. Arc welding usually produces a large heat affected zone (HAZ), which leads to lower joint strength on aluminium alloys. AA7075 aluminium alloy has many advantages due to its light weight, low density, high corrosion resistance, and high alloy strength as compared to steel. This paper presents a weld feasibility studies on AA7075 surface using low power fiber laser with two different modes; continuous wave (CW) and pulse wave (PW) modes. The intention of this research work is to investigate the effect of laser welding modes with different focal position on penetration depth, type of weld penetration, and microstructure of bead on plate welded AA 7075 using low power fiber laser. The bead-on-plate (BOP) welding was carried out by heating the surface of AA7075 with a thickness of 2 mm using both CW and PW modes with focal lengths that ranged from 60 to 200 mm. 90 % power was used for both welding modes with the same welding speed, 2 mm/s. The macrostructure of the welded line was captured using an optical microscope, and the beam width and penetration were measured. The smallest bead was observed at 120 mm focal length with 570 µm diameter. Pulse wave (PW) welding with keyhole profile produced optimum penetration depth, which was approximately 1.0 mm. However, continuous mode (CW) welding produced 0.153 mm penetration depth. To conclude, AA 7075 could be joined using the low power fiber laser welding method since the half weld penetration with keyhole profile was produced. For better welding joint with fewer defects, shielding gas and incident angle of laser beam could be applied.

***Keywords:*** AA 7075; fiber laser; BOP; laser modes; optimum depth; microstructure.

## INTRODUCTION

A joining process could be classified in different ways such as mechanical and welding joining. To join aluminium alloys, conventional arc welding such as Metal Inert Gas (MIG), Tungsten Inert Gas (TIG) and Resistance Spot Weld (RSW) and solid state welding such as Friction Stir Welding (FSW) are used [1-9]. With new developments in welding technology, laser welding has been introduced into the industrial world. There are several typical types of laser used in industries such as Diode, Neodymium-doped: Yttrium Aluminium Garnet (Nd:YAG), Carbon Dioxide ($CO_2$), and fiber laser. However, fiber laser is observed to be the finest type to be applied in the welding industry [10]. Fiber laser welding is usually selected due to its low cost maintenance compared to other solid state

laser and $CO_2$ laser [11]. Furthermore, the cost can be reduced by using low power fiber laser machine, which could be of great advantage, especially for the transportation industry when light weight vehicles are produced, which automatically increases fuel efficiency.

Aluminium alloys has lower density, which is 1/3 of that of steel and it has strong mechanical properties. AA7075 aluminium alloys was chosen in this study since there are not many studies on welded by fiber laser welding method and its application remains obscure [4, 8, 12-15]. The 7000 series is a typical heat-treated alloys which can be categorized into high strength Al-Mg-Mg-Cu type, represented by AA7050 and AA7075, where the principle added elements used are Al-Zn-Mg [16]. The weldability of aluminium alloys in terms of weld penetration when welded by low power fiber laser is the significance of this study. In addition, this method can replace conventional arc welding since there is no filler metal used to affect density. Many researches used high power laser with continuous wave mode to produce weld joint, which contributes to high cost including maintenance, although only to weld 2 mm thickness metal [17-20].

In a study by previous researchers, a 10kW fiber laser was used to weld 1XXX , 5XXX, 6XXX, and 7XXX series aluminium alloys of 10 mm thickness [21]. Nd:YAG laser with 2200 Watt maximum power and fiber laser with of 4000 Watt maximum power were used to weld similar joint of AA 7075 [22, 23]. In this research, we used a low power fiber laser, which has as low as 200 Watt maximum average power. Laser welding of aluminium alloys is difficult due to their high reflectivity and heat conductivity compared to ferrous metal [18]. However, laser welding can form a keyhole penetration profile, in which the heat affected zone (HAZ) is smaller, and can produce a strong weld joint. The focus point plays an important role since it can affect the peak power density of laser, which is measured by a beam profiler [21]. Spot diameter contains the energy of a laser light, which is equivalent to the Gaussian distribution ($1/e^2$) [18]. This paper reports the effects of welding mode, pulse and continuous on the penetration depth, type of penetration, and microstructure of BOP welded AA7075 using low power fiber laser as a feasibility study to weld aluminium alloys.

## EXPERIMENTAL SETUP

### Experimental Procedure

AA7075 was prepared with a dimension of 100 mm x 100 mm and 2 mm thickness using shearing cutting machine. The chemical composition of AA7075 parent metal was checked using spectrometer and the composition is listed in Table 1.

Table 1. Chemical composition of AA7075.

| Elements | Al | Zn | Mg | Cu | Fe | Si | Mn |
|---|---|---|---|---|---|---|---|
| Compositions (wt.%) | 89.8 | 5.58 | 2.28 | 1.6 | 0.27 | 0.07 | 0.02 |

Ytterbium Laser Machine-Quasi Continuous Wave (YLM-QCW) fiber laser machine with wavelength ranged at 1.0 µm was used. The maximum average power was 200 Watt with peak power of 2 kW for pulse mode (PW) and continuous mode (CW). The bead-on-plate welding was carried out using both welding modes. The angle of irradiation was 0°. The weld width was measured from the sample surface for all BOP welded line. The welded sample was then cut using a cut-off machine and hot mounted to produce the welded cross-section part. The welded sample then was prepared through

grinding, polishing and etching processes. The etching process was very important in order to reveal the microstructure of AA7075. Keller's Reagent solution was used for the etching process and its composition is shown in Table 2. The penetration depth was measured from the welded cross section and the microstructure was observed by optical microscope (OM)., The microstructural behaviour of the welded sample was analysed from the metallographic observation.

Table 2. Keller's reagent composition.

| Chemical element | Volume (ml) |
|---|---|
| Water ($H_2O$) | 94 |
| Nitric Acid ($HNO_3$) | 5 |
| Hydrochloric Acid (HCl) | 3 |
| Hydrofluoric Acid (Hf) | 2 |

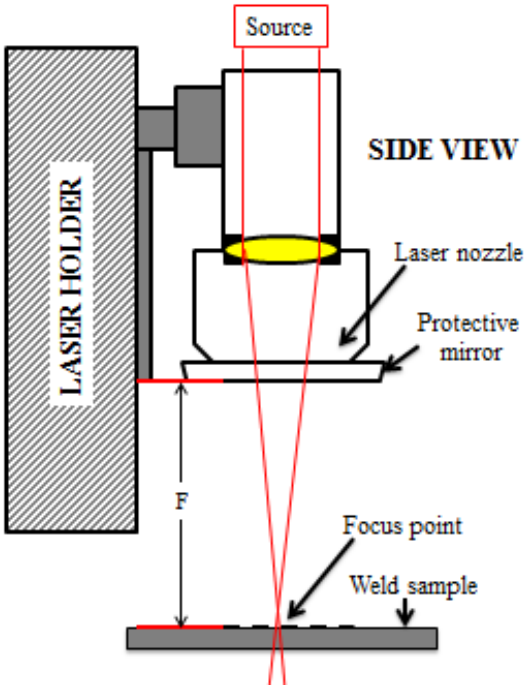


Figure 1. Fiber laser BOP welding setup.

**Experimental Design**

In this experimental study, both PW and CW modes were selected for the fiber laser. The parameters for this laser such as power percentage (W), pulse width (ms), pulse repetition rate (Hz), and welding speed (mm/s) remained constant. The variable parameter is the focal length (mm). The welding configuration is shown in Figure 1. Referring to Figure 1, the focal length datum was measured from the sample surface to the protective mirror. Table 3 presents the selective parameter to conduct the BOP welding using low power fiber laser. Figure 2 shows the method to analyse the weld width on the welded AA7075 surface and the weld penetration depth. The smallest weld width was concluded as the focus point. The highest depth of penetration was concluded as the optimum depth at the optimum focal position. Welded samples were prepared through grinding, polishing, and etching process to reveal the microstructure. The microstructure of both welded samples

using CW and PW modes were observed and analysed in term of grain sizes, grain boundaries, and penetration produced.

Table 3. Bead-on-Plate laser welding parameters.

| Parameter | Pulse Mode (PW) | Continuous Mode (CW) |
|---|---|---|
| Power (Watt) | 1800 W (90%) | 180 W (90%) |
| Welding Speed (mm/s) | 2mm/s | |
| Pulse Width (ms) | 1 ms | - |
| Pulse Repetition Rate (Hz), PRR | 20 Hz | - |
| Focal Length (mm), F | 60 mm – 200 mm | |

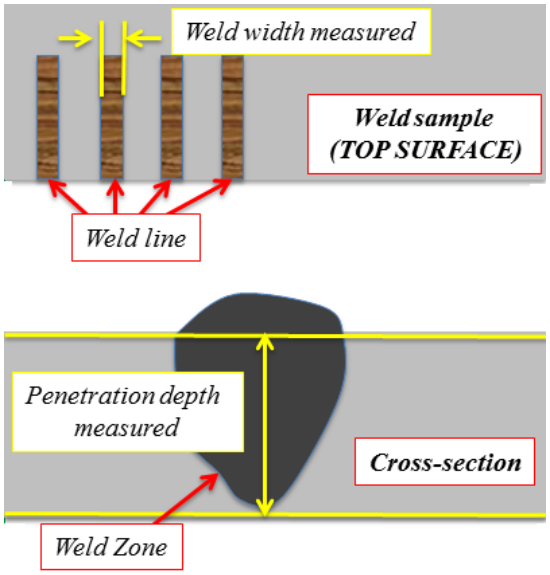


Figure 2. Weld width and depth of penetration analysis.

## RESULTS AND DISCUSSION

### Weld Width Analysis and Penetration Depth

Fifteen weld lines were made for both welding modes. Figure 3 and Figure 4 show images of the welded line produced through BOP laser welding for PW and CW modes, respectively. The weld width and depth of penetration measurements for both welding condition are tabulated in Table 4. The penetration depth was measured from the sample cross-section obtained from the optical microscope. Based on Figure 3, it was observed that at focal length, F= 100 mm, good weld appearance was produced compared to the weld produced at focal lengths ranging from 110 mm to 140 mm. This is due to higher energy absorption during PW mode welding as the focal length achieved the focus point on the metal surface [24]. It was shown that starting from F = 150 mm, the weld line became unclear and no weld line was observed when the focal length was greater than 180 mm since laser beam had already defocused at these focal lengths.

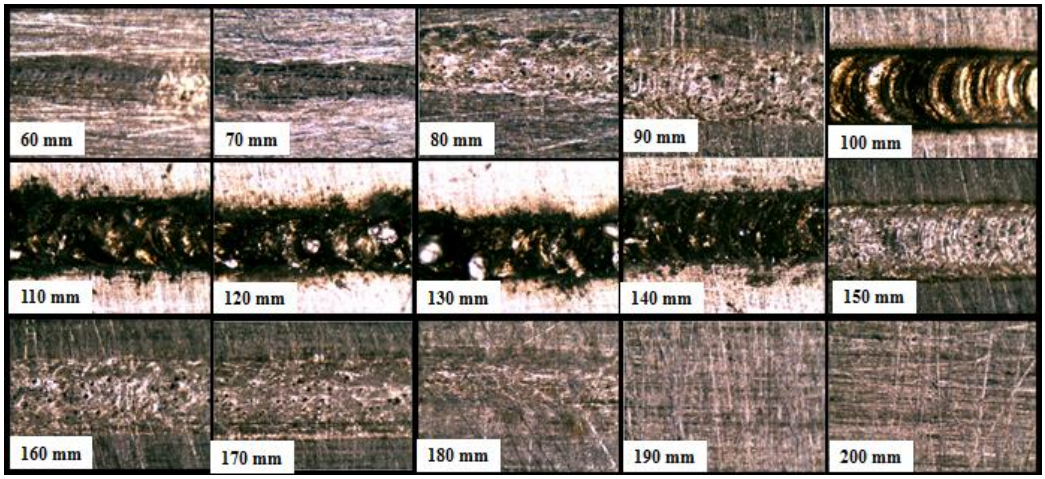


Figure 3. Weld line produced on sample surface (PW) with different focal lengths.

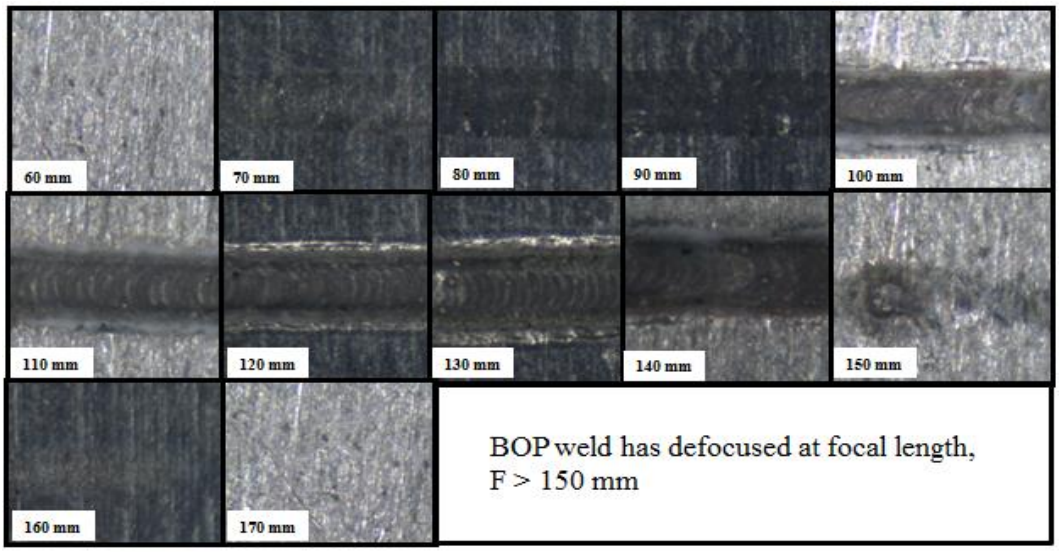


Figure 4. Weld line produced on sample surface (CW) with different focal lengths.

Based on Figure 4, it was found that weld line could not be obtained at F=150 mm and above using CW welding mode compared to the PW welding mode. This is because the laser power produced by PW was greater than the power produced by CW, since PW had its high peak power at 1.8 kW [25]. From Table 4, it was found that the smallest weld width (bead width) was obtained at the focal length, F=120 mm for both welding modes with 570 µm and 417 µm for PW and CW modes, respectively. Both welding modes produced different weld width. This is due to the different values of laser power, hence producing different energy. As shown in Table 4, the largest weld width was measured at focal length 180 mm with 785 µm using PW welding mode. No weld line was observed at focal lengths higher than 190 mm and 150 mm for PW and CW, respectively. It was observed the further away the focal length from the focus, the laser beams defocused due to larger laser beam width. This situation was also the same for focal lengths below 60 mm. For PW mode, pulsed energy plays an important role, whereby the power intensity produced was higher compared to CW mode. This is because CW mode does not have peak power since it only produces average laser power during the welding process. It was

concluded that the focus point of the laser machine on AA 7075 surface was at F=120 mm.

Table 4. Weld width and penetration depth results.

| Focal Length (mm) | Weld Width (µm) | | Penetration depth (mm) | |
|---|---|---|---|---|
| | PW Mode | CW Mode | PW Mode | CW Mode |
| 60 | 617 | defocussed | 0.030 | defocussed |
| 70 | 626 | 454 | 0.040 | Non-observed |
| 80 | 660 | 484 | 0.120 | 0.061 |
| 90 | 699 | 516 | 0.130 | 0.111 |
| 100 | 703 | 547 | 0.134 | 0.173 |
| 110 | 727 | 478 | 0.450 | 0.140 |
| 120 | 570 | 417 | 0.990 | 0.153 |
| 130 | 589 | 492 | 0.970 | Non-observed |
| 140 | 687 | 523 | 0.230 | Non-observed |
| 150 | 668 | defocussed | 0.140 | defocussed |
| 160 | 734 | defocussed | 0.100 | defocussed |
| 170 | 832 | defocussed | 0.040 | defocussed |
| 180 | 785 | defocussed | 0.050 | defocussed |
| 190 | defocussed | defocussed | 0.007 | defocussed |
| 200 | defocussed | defocussed | 0.012 | defocussed |

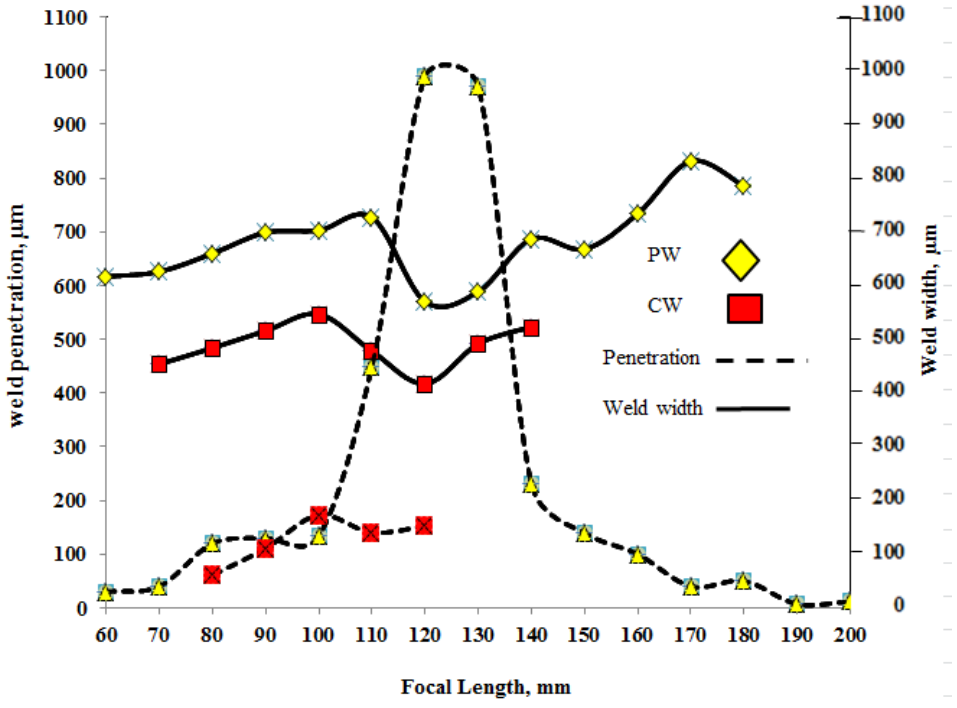


Figure 5. Weld width/weld penetration vs focal length.

Figure 5 shows a graph of the weld width and depth of penetration versus focal length. From the graph, it was clearly observed that both welding modes produced focus position at the same focal length, F=120 mm. It proved that the laser beam has a focus

point at a focal length of 120mm due to the smallest beam diameter produced for both welding modes. From the result, it was observed that PW mode produced the highest depth of penetration at the focus point, F with 0.99 mm or half of AA7075 sample compared to CW mode, which only produced 0.173 mm as the highest at F=100 mm. This is due to the differences in the laser power since PW can produce peak power of 2.0 kW compared to CW, which only produces maximum average power of 200 W. Higher laser power can produce better penetration due to higher heat input and higher efficiency to make a weld joint with keyhole profile. In addition, PW has different pulsed energy to produce different weld penetration as pulsed laser is pumped at high intensity for a short period of time. This is due to the different power densities produced to the metal [26]. PW mode was also proved to be a better welding mode as it reduces porosity with higher weld penetration with smaller grain size produced in the weld zone compared to CW [25].

**Microstructure analysis**

After the BOP laser welding process, the cross section of the welded samples selected from the optimum depth for both welding modes was compared as shown in Figure 6. It was found that PW produced a narrow and deep penetration (keyhole profile) compared to CW, which could only produce wider weld zone and low penetration depth (conduction profile). From Figure 6 (a), it was observed that the keyhole profile was produced at 0.99 mm depth, which is half of the sample thickness, 2 mm. However, underfill was present as defects because there shielding gas was not used in this experiment, where it could not protect the molten pool during the welding process. Keyhole was present when the vapour plume during the laser welding process open the keyhole in the molten pool in a short time period [27]. Figure 6(b) shows that CW produced a conduction profile with 0.173 mm of penetration depth. It was found that porosity occurred at the welded zone of the sample welded with CW mode, as shielding gas was not used. From the microstructural analysis, it was observed that PW welding mode produced a good weld joint compared to CW mode in term of weld seam profile, which contributes to a stronger welding joint. With low fibre laser welding machine, a half depth penetration was achieved for 2 mm thickness aluminium alloys. Double-sided welding method can also be selected, which can produce stronger weld joint compared to one-side penetration for 2 mm thickness AA7075.

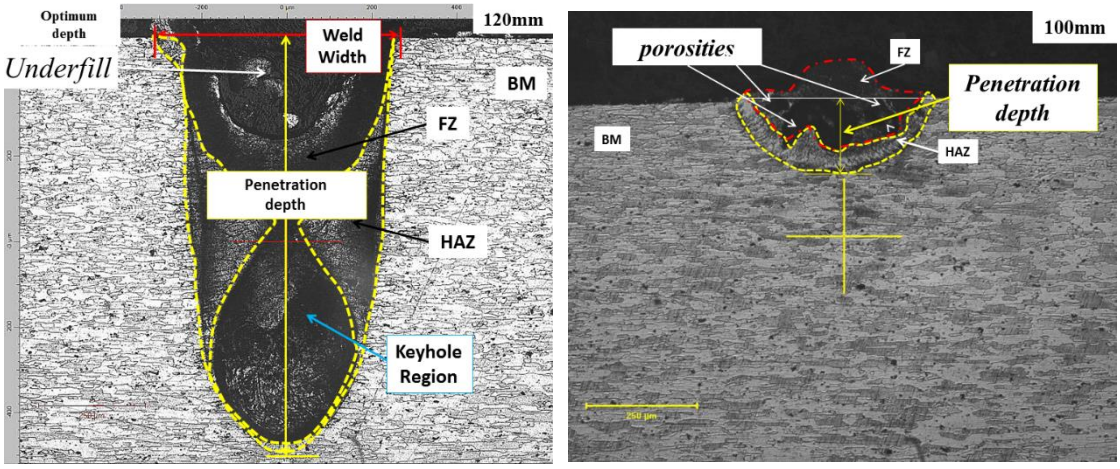


(a) (b)

Figure 6. AA7075 BOP laser welded (a) PW (b) CW (10 x magnifications).

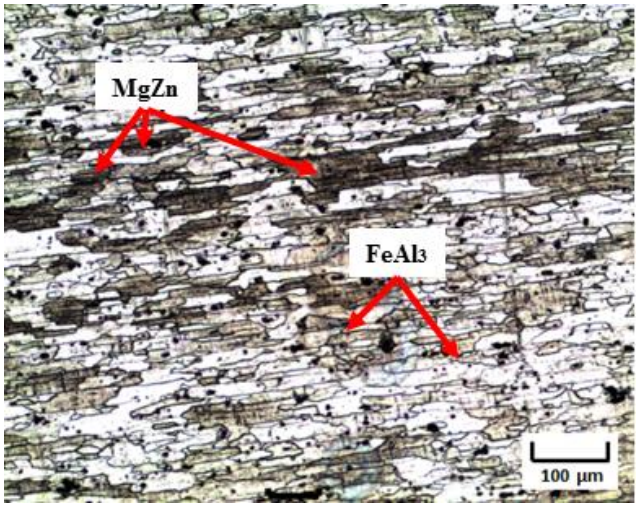


Figure 7. AA7075 base metal (10 x magnification).

The microstructure for base metal AA7075 shows spheroidal particles of black precipitate MgZn with light grey $FeAl_3$ particles [28] as shown in Figure 7, which are present in aluminium solid solution. It was observed that the grains elongated horizontally in one direction. It was observed that the element presented in the base metal was proven to be Al, Mg, and Zn elements with a small amount of Fe element.

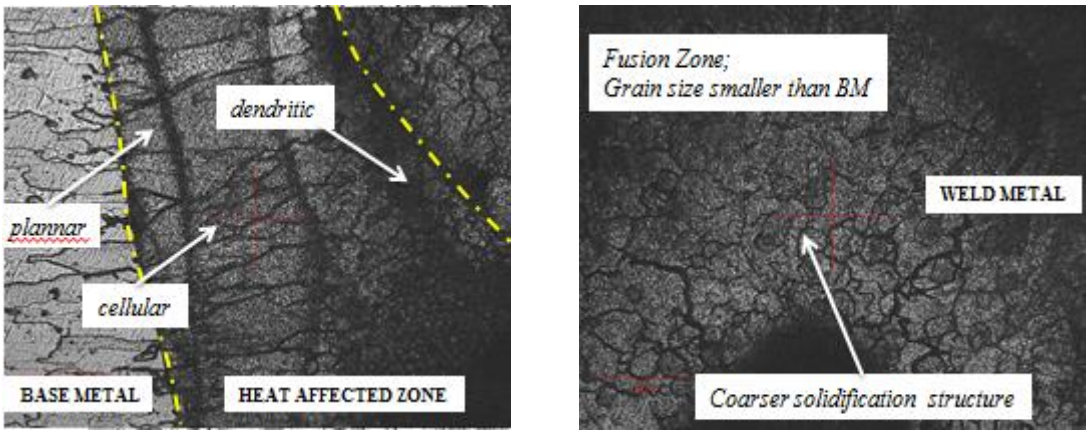


(a) (b)

Figure 8. Microstructure of the sample welded by PW (keyhole) at (a) PMZ (b) Weld zone.

The best weld result was selected in order to discuss about the microstructure. Figure 8 (a) shows the microstructure changing from the base metal to weld metal through the partially melted zone (PMZ). The elongated grain structure started to change into planar grain structure at the HAZ transition line because it was affected by the heat from the laser source and turned into cellular grain structure at the centre of HAZ [29]. Dendritic grain structure was observed at the transition line between HAZ and weld zone due to the high amount of heat produced [30]. The hardness at HAZ was lower compared to BM as it is normally fractured at this point. From Figure 8 (b), it was found that coarser dendritic grain structure formed and the grain size was smaller compared to the grain size

of the base metal with an average value of grain size are 63.6 µm and 18.3 µm for base metal and weld zone, respectively.

## CONCLUSIONS

From this study, it was proved that the weld joint of AA7075 sheet metal can be produced using low power fiber laser. The following points were concluded from this experiment;

i). PW welding mode showed significant result with keyhole penetration observed from the cross-section microstructure approximately 1 mm penetration depth compared to the CW mode. Weld joint can be produced as half penetration depth was achieved.
ii). Both welding mode showed the same result for the focused point. The focused point measured from the sample surface to the protective mirror was at F = 120 mm.
iii). The microstructure changed from elongated grain in the base metal into dendritic grain in the weld zone. Defects such as underfill and porosity occurred because no shielding gas was used during the experiment.

Low power fiber laser could be applied to weld high strength aluminium alloys such as AA 7075. This method can participate successfully in the automotive industry. This metal can be a replacement for conventional steel used for car body panel in automotive parts, or Taylor Welded Blanks (TWBs) application. For future recommendation, laser parameters such as shielding gas, incident of beam angles, and pulsed energy could be studied using design of experiment (DOE) for better weld result in welding AA 7075.

## ACKNOWLEDGEMENTS

The author would like to thank the technical staff of Universiti Malaysia Pahang for all of the work by providing laboratory facilities within which the experiments were conducted. Also, financial support by the Ministry of Education through Universiti Malaysia Pahang for research grant RDU140118 is gratefully acknowledged.

## REFERENCES

[1] Shah LH, Akhtar Z, Ishak M. Investigation of aluminum-stainless steel dissimilar weld quality using different filler metals. International Journal of Automotive and Mechanical Engineering. 2013;8:1121-31.
[2] Ghazali FA, Manurung YHP, Mohamed MA, Alias SK, Abdullah S. Effect of process parameters on the mechanical properties and failure behavior of spot welded low carbon steel. Journal of Mechanical Engineering and Sciences. 2015;8:1489-97.
[3] Ishak M, Islam MR, Sawa T. GMA Spot welding of A7075-T651/AZ31B dissimilar alloys using stainless steel filler. Materials and Manufacturing Processes. 2014;29:980-7.
[4] Ishak M, Noordin NFM, Razali ASK, Shah LHA, Romlay FRM. Effect of filler on weld metal structure of AA6061 aluminum alloy by tungsten inert gas welding.

International Journal of Automotive and Mechanical Engineering. 2015;11:2438-46.

[5] Shah LH, Mohamad UK, Yaakob KI, Razali AR, Ishak M. Lap joint dissimilar welding of aluminium AA6061 and galvanized iron using TIG welding. Journal of Mechanical Engineering and Sciences. 2016;10:1817-26.

[6] Sathari NAA, Razali AR, Ishak M, Shah LH. Mechanical strength of dissimilar AA7075 and AA6061 aluminum alloys using friction stir welding. International Journal of Automotive and Mechanical Engineering. 2015;11:2713-21.

[7] Hasan MM, Ishak M, Rejab MRM. A simplified design of clamping system and fixtures for friction stir welding of aluminium alloys. Journal of Mechanical Engineering and Sciences. 2015;9:1628-39.

[8] Ahmad R, Asmael MBA. Effect of aging time on microstructure and mechanical properties of AA6061 friction stir welding joints. International Journal of Automotive and Mechanical Engineering. 2015;11:2364-72.

[9] Sathari NAA, Shah LH, Razali AR. Investigation of single-pass/double-pass techniques on friction stir welding of aluminium. Journal of Mechanical Engineering and Sciences. 2014;7:1053-61.

[10] Assunção E, Quintino L, Miranda R. Comparative study of laser welding in tailor blanks for the automotive industry. The International Journal of Advanced Manufacturing Technology. 2009;49:123-31.

[11] Tsuji M. IPG fibre lasers and aluminium welding applications. Welding International. 2009;23:717-22.

[12] Ahmad AH, Naher S, Brabazon D. Effects of cooling rates on thermal profiles and microstructure of aluminium 7075. International Journal of Automotive and Mechanical Engineering. 2014;9:1685-94.

[13] Singh R. Process capability study of rapid casting solution for aluminium alloys using three dimensional printing. International Journal of Automotive and Mechanical Engineering. 2011;4:397-404.

[14] Kadirgama K, Noor MM, Rahman MM, Rejab MRM, Haron CHC, Abou-El-Hossein KA. Surface roughness prediction model of 6061-T6 aluminium alloy machining using statistical method. European Journal of Scientific Research. 2009;25:250-6.

[15] Najiha MS, Rahman MM, Kadirgama K, Noor MM, Ramasamy D. Multi-objective optimization of minimum quantity lubrication in end milling of aluminum alloy AA6061T6. International Journal of Automotive and Mechanical Engineering. 2015;12:3003-17.

[16] Fukuda T. Weldability of 7000 series aluminium alloy materials. Welding International. 2012;26:256-69.

[17] Katayama S, Ogawa K. Laser weldability and ageing characteristics of welds: laser weldability of commercially available A7N01 alloy (1). Welding International. 2013;27:172-83.

[18] Kawahito Y, Matsumoto N, Abe Y, Katayama S. Laser absorption of aluminium alloy in high brightness and high power fibre laser welding. Welding International. 2012;26:275-81.

[19] Moon J, Katayama S, Mizutani M, Matsunawa A. Behaviour of laser induced plasma, keyhole and reflected light during laser welding with superimposed beams of different wavelengths. Welding International. 2003;17:524-33.

[20] Ishak M, Yamasaki K, Maekawa K. Lap fillet welding of thin sheet AZ31 magnesium alloy with pulsed Nd:YAG Laser. Journal of Solid Mechanics and Materials Engineering. 2009;3:1045-56.
[21] Katayama S, Nagayama H, Mizutani M, Kawahito Y. Fibre laser welding of aluminium alloy. Welding International. 2009;23:744-52.
[22] Enz J, Riekehr S, Ventzke V, Sotirov N, Kashaev N. Laser welding of high-strength aluminium alloys for the sheet metal forming process. Procedia CIRP. 2014;18:203-8.
[23] Wang JT, Zhang YK, Chen JF, Zhou JY, Ge MZ, Lu YL, et al. Effects of laser shock peening on stress corrosion behavior of 7075 aluminum alloy laser welded joints. Materials Science and Engineering: A. 2015;647:7-14.
[24] Katayama Seiji AY, Mizutani Masami, Kawahito Yousuke. Deep Penetration Welding with High-Power Laser under Vacuum. Transactions of JWRI is published by Joining and Welding Research Institute, Osaka University, Ibaraki, Osaka 567-0047, Japan. 2011;40.
[25] Jiang Z, Tao W, Yu K, Tan C, Chen Y, Li L, et al. Comparative study on fiber laser welding of GH3535 superalloy in continuous and pulsed waves. Materials & Design. 2016;110:728-39.
[26] Esraa K. Hamed FH, Makram Fakhry. Laser wavelength and energy effect on optical and structure properties for nano titanium oxide prepared by pulsed laser deposition. Iraqi Journal of Physics. 2014;12:62-8.
[27] Pang S, Chen X, Shao X, Gong S, Xiao J. Dynamics of vapor plume in transient keyhole during laser welding of stainless steel: Local evaporation, plume swing and gas entrapment into porosity. Optics and Lasers in Engineering. 2016;82:28-40.
[28] Sivashanmugam NMM, D. Ananthapadmanaban, S. Ravi Kumar. Investigation of microstructure and mechanical properties of GTAW and GMAW joints of AA7075 aluminium alloys International Journal on Design and Manufacturing Technologies. 2009;2:56-62.
[29] Chen S, Guillemot G, Gandin C-A. Three-dimensional cellular automaton-finite element modeling of solidification grain structures for arc-welding processes. Acta Materialia. 2016;115:448-67.
[30] Dong HB. Analysis of Grain Selection during Directional Solidification of Gas Turbine Blades. In: 2007 W, editor. Proceedings of the World Congress on Engineering 2007 Vol II, London, UK2007.